RECENT UPDATES TO THE OPTICAL PROPAGATION CODE OPC

P.J.M. van der Slot#
Mesa+ Institute for Nanotechnology, University of Twente, Enschede, The Netherlands
Department of Electrical and Computer Engineering, Colorado State University, Fort Collins, USA
K.-J. Boller
Mesa+ Institute for Nanotechnology, University of Twente, Enschede, The Netherlands

Abstract

In order to understand and design free-electron lasers (FELs), simulation codes modeling the interaction of electrons with a co-propagating optical field in the magnetic field of an undulator are essential. However, propagation of the optical field outside the undulator is equally important for evaluation of the optical field at the location of the application or to model FEL oscillators.

The optical propagation code OPC provides such capabilities and can interface with FEL gain codes like GENESIS 1.3, MEDUSA and MINERVA. Here we present recent additions and modifications to the code that improves the speed of the code and extends the modeling capabilities. These include amongst other, inline diagnostics that results in considerable faster runtimes, the ability to convert from free-space modes to guided modes (currently only cylindrical waveguides), and the possibility to determine the spectrum at each transverse location. The latter opens the possibility to include dispersion in the optical propagation.

INTRODUCTION

Simulation tools play an essential role in the design and understanding of free-electron lasers (FELs). In the last few decades, several codes have been developed to model the interaction of electrons with a co-propagating optical field inside the magnetic field of an undulator, amongst others, GENESIS 1.3 [1], GINGER[2], MEDUSA [3] and MINERVA [4] as a recent addition. These codes are used to calculate the spatio-temporal characteristics of the optical pulse coming out of the undulator. However, self-consistent modelling of an oscillator FEL also requires to model the propagation of the optical pulse outside the gain section, i.e., outside the undulator. Even for single pass systems, a system designer or user is typically interested in the characteristics of the optical pulse in the far field. The optical propagation code (OPC) [5] provides tools for propagating the optical field outside the gain section and interfaces with the FEL gain codes GENESIS 1.3, MEDUSA and MINERVA. The main properties of OPC are described in ref. [5], and we only summarize its main characteristics here. The propagation of the optical field is done using one of three methods, a spectral method, a Fresnel diffraction integral and a modified Fresnel diffraction integral. These methods propagate the complex phasor of the electric field of the optical pulse from an input plane to an output plane, where the modified Fresnel integral allows for an expansion of the grid on which the optical field is defined, but not the number of grid points. OPC allows placement of various optical elements along the propagation path, such as apertures, lenses and mirrors. In this paper we describe the recent additions to the code that enhances its capabilities and increases the speed of the code. The remainder of the paper is organized as follows. We will first describe the addition of inline diagnostics, which is then followed by a description of waveguide modes and finally we discuss the possibility to propagate in the frequency domain, which allows the use of dispersive elements in the optical path. We conclude with a brief summary and outlook for future additions to OPC.

IN-LINE DIAGNOSTICS

In order for the user to analyze the optical properties of the light generated in the FEL, the user has the ability to execute a number diagnostics on the optical pulse, such as obtaining the intensity $I(x,y,s)$ as a function of the position (x,y) in the transverse plane for a specific longitudinal position s, the phase $\Theta(x,y,s)$ as a function of the position (x,y) for a specific s or $\Theta(x=x_0,y=y_0,s)$ as a function of s for a specific transverse location (x_0,y_0), the power $P(s)=\iint I(x,y,s)dxdy$ in the pulse, the fluence $F(x,y)=\int I(x,y,s)ds$, a cross section $I(x,y=y_0,s)$ or $I(x=x_0,y,s)$ through the pulse, the "centre of gravity" (x_c,y_c) of the optical pulse and its rms radius r_{rms} (weighted with the intensity distribution). These diagnostics can be applied at any (intermediate) plane along the optical path where the optical field is evaluated. Until recently, OPC first propagates the optical from start to end of the optical path, while storing the optical field at the locations where diagnostics are requested. After the optical propagation has completed, the user can perform the diagnostic commands to the stored optical field. For this reason, we refer to this as off-line diagnostics.

The stored optical field consists of the complex phasor (amplitude and phase) of a linearly polarized electric field at each grid point for each of the time samples of the optical field, and the amount of data can become very large for large grid sizes ($N_x \times N_y = N_p^2$, for simplicity) and/or number of times samples N_s. For this reason, the optical field is stored on disk and the associated disk I/O can have an impact on the speed of the program when the files become large or a large number of diagnostics are requested.

#p.j.m.vanderslot@utwente.nl

ISBN 978-3-95450-133-5

To avoid a significant increase in run time due to diagnostic evaluations wanted by the user, OPC has been upgraded with so-called in-line diagnostics. Instead of dumping the optical field to the hard disk when diagnostics are requested, the user can now execute diagnostic commands during the propagation along the optical path. These new diagnostics commands are applied to the optical field while it is still in the memory of the computer and therefore avoids a large amount of relative slow disk I/O. Backward compatibility with off-line diagnostics is maintained to allow the user to use earlier work without modifications and to post-process optical fields produced at an earlier time.

In order to obtain an impression about the speed improvement, we created a script that times the speed of the calculations in three cases. In the first, a predefined optical field is propagated over a distance of 5 m using the Fresnel diffraction integral method. This provides the time t_p required to do the propagation. In the second case, the predefined field is again propagated using the same method and at the end of the path the optical field is dumped and processed with a diagnostic command after the propagation is completed (off-line diagnostic). This provides the time t_{pod} for the propagation and off-line diagnostic command. The third and last case propagates the same predefined optical field but now implements the same diagnostic command at the end of the propagation path (in-line diagnostic). This provides the time t_{pid} of the propagation plus the in-line diagnostic command. Each case is executed 20 times consecutively, to obtain an average execution time. The tests were run on a duo Xeon computer with a total of 12 cores. The results are summarized for the diagnostic commands total and statistics in Tables 1 and 2 for $N_s = 300$ and $N_s = 600$ time samples, respectively. The command to generate a cross section through the intensity profile shows a similar behavior.

Table 1: Average Execution Time for the Diagnostic Commands Total and Statistics, $N_s = 300$

		total		statistics	
N_p	t_p (s)	t_{pod} (s)	t_{pid} (s)	t_{pod} (s)	t_{pid} (s)
255	2.0	3.2	2.0	3.1	2.0
441	3.5	4.6	3.3	4.6	3.3
567	4.9	6.2	4.8	6.3	4.7
945	11.9	20.0	11.6	19.2	11.7

Table 2: Average Execution Time for the Diagnostic Commands Total and Statistics, $N_s = 600$

		total		statistics	
N_p	t_p (s)	t_{pod} (s)	t_{pid} (s)	t_{pod} (s)	t_{pid} (s)
255	2.4	4.1	2.9	3.1	2.0
441	5.8	7.1	5.3	7.1	5.3
567	8.8	16.2	8.2	20.6	8.4
945	22.0	57.1	49.9	61.6	51.6

The results in Table 1 show that a single in-line diagnostics command hardly effects the runtime of the code compared to a single propagation step, while a single off-line diagnostic command can almost double the runtime of a single propagation step. Table 2 shows the runtimes when we increase the number of time samples from N_s=300 to N_s=600. For the three smallest number of grid points (N_p = 255, 441 and 567), a single in-line diagnostic command again hardly increase the run time while a single off-line diagnostic command can more than double the run time. Only for the combination of the largest value for N_p = 945 and N_s = 600, we observe a serious degradation in performance for the in-line diagnostics, although they still outperform the equivalent off-line diagnostic command. Note, for these parameters (N_p = 945 and N_s=600), the optical field corresponds to almost 9 GB of data.

WAVEGUIDE MODES

When the FEL emits light at THz or longer wavelengths, the natural diffraction of the light becomes so large that the effect of the vacuum tube, through which the electrons move, cannot be neglected any more. The electromagnetic wave becomes guided. The MINERVA gain code [4] will be able to model FELs with guided or partial guided wave propagation inside the undulator. In order to support cold cavity calculations and propagate the optical field back to the entrance of the undulator, OPC has been extended to include waveguide modes. Currently only cylindrical waveguides modes are supported.

An additional "*waveguide*" option as part of the optical path has been made available to the user. This option decomposes an incident optical field in free space into waveguide modes and obtains the complex phasor (amplitude and phase) for each mode [6]. These modes are then propagated to the other end of the waveguide, where they are combined into a new optical field that is emitted into free space. Typically, the wavelength is sufficiently far below the cut-off wavelength that reflection at the waveguide end can be neglected [6]. The user has access to the modal decomposition and obtain the energy and amplitude for each of the excited modes. Although one may start with a linear polarized optical field in free space, the optical field will possess two orthogonal polarization directions after propagating through a cylindrical waveguide. OPC has been extended to include two perpendicular polarizations to accurately model the optical field emitted into free space from a waveguide. This framework can in principle also be used to propagate circular polarized light along an optical path. As an example, Fig. 1 shows how much power is coupled in the fundamental TE_{11} mode and all TE modes together as a function of the waist w_0 of a fundamental Gaussian TEM_{00} mode when it is focused on the end of a cylindrical waveguide with an inner radius R_{wg} = 3 mm. Note, as the peak intensity of the incident TEM_{00} mode is kept constant, the total power in the incident field increases with the size of the focus. As the waist of the TEM_{00} mode increases from its minimal value of 1 mm, more power is coupled into the waveguide and between w_0 = 2 and 2.4 mm less than 1 % of the coupled power is

ISBN 978-3-95450-133-5

in higher order modes. At optimum coupling, w_0 is 2.4 mm and 87.5 % of the incident power is coupled into the fundamental TE_{11} mode. When the waist is further increased, less power is coupled into the waveguide and higher order modes are excited. This is because the incident optical field becomes too large and a considerable fraction of the field falls outside the aperture provided by the cylindrical waveguide.

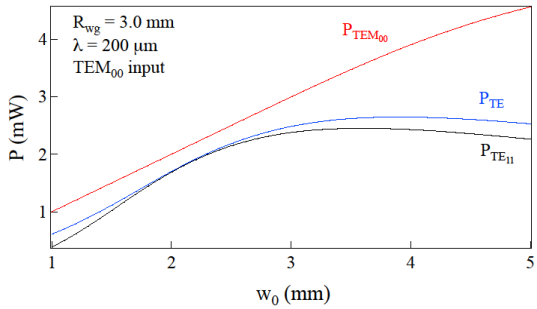

Figure 1: Coupling between free-space Gaussian TEM_{00} mode and the TE_{nm} modes in a cylindrical waveguide of radius R_{wg} = 3 mm.

SPECTRAL DOMAIN

Until recently, OPC assumed that the optical bandwidth of the pulse is sufficiently small that the center wavelength of the optical field can be used for the propagation and that dispersion along the optical path is not important. These assumptions break down when (ultra)short pulses need to be propagated or when the optical components used along the optical path have a significant dispersion over the bandwidth of the optical pulse. OPC has been upgraded to give the user the choice to propagate in the time domain where consecutive time samples are propagated one after the other along the optical path (using the center wavelength), or to transfer to the frequency domain where consecutive frequencies are propagated along the optical path.

The transformation to the frequency domain also allows users to inspect the transverse distribution of the various frequency components. As an example we show in Fig.2 the energy at the exit of the undulator of an FEL oscillator [7] as a function of the roundtrip number. The system parameters are listed in the figure. Figure 2 suggests that the system becomes stationary, i.e., no changes from one pass to the next, after about 400 roundtrips. The power of the optical pulse as a function of the roundtrip n and the longitudinal internal coordinate $s = ct$, where c is the speed of light in vacuum and t is the time coordinate, is shown in Fig. 3 and although the pulse energy is almost constant, the temporal shape of the pulse still changes after n = 400. The spectrum of the optical pulse at n = 900 roundtrips is shown in Fig.4. As the initial carrier wavelength was at 495 nm, Fig. 4 shows that the wavelength with maximum spectral energy density is at

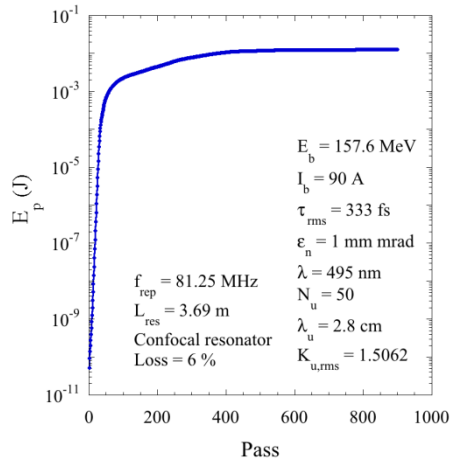

Figure 2: Pulse energy at the exit of the undulator in a FEL oscillator as a function of the roundtrip number.

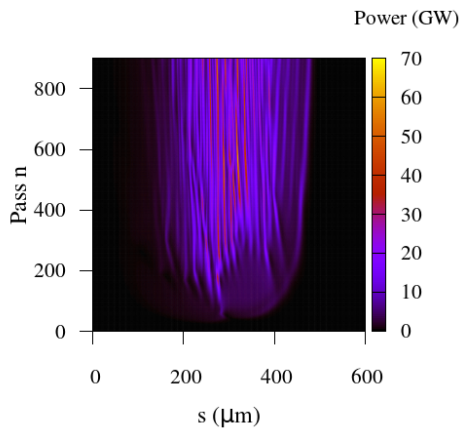

Figure 3: Power $P(n, s)$ as a function of the roundtrip number n and the internal longitudinal coordinate $s = ct$ for the parameters of Fig. 2.

499.8 nm, while the intensity weighted average wavelength is $\bar{\lambda}$ = 521 nm, where $\bar{\lambda}$ is defined as

$$\bar{\lambda} = \frac{\int \lambda I(\lambda) d\lambda}{\int I(\lambda) d\lambda} \quad (1)$$

The rms bandwidth is defined as

$$\Delta\lambda_{rms} = \sqrt{\overline{\lambda^2} - \bar{\lambda}^2}, \quad (2)$$

where $\overline{\lambda^2}$ is defined similar as $\bar{\lambda}$. For the spectrum shown in Fig. 4, we find that $\Delta\lambda_{rms}$ = 35 nm. Note, the -3 dB bandwidth $\Delta\lambda_{-3dB}$ = 0.81 nm.

OPC also provides the possibility to inspect the transverse energy distribution of the frequency components. Examples are shown in Fig. 5, where we plot the transverse distribution for the initial carrier wavelength (495 nm), the wavelength with the highest spectral energy density (499.8 nm), close to the average wavelength (521.3 nm) and an arbitrary wavelength (530.2 nm).

ISBN 978-3-95450-133-5

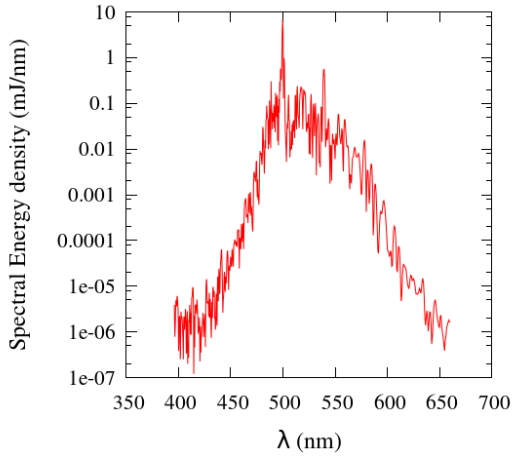

Figure 4: Spectrum of the optical pulse after 900 roundtrips. Parameters as in Fig. 2.

Figure 5 shows that not all frequency components in the spectrum have the same transverse distribution. For example, not all frequency components have their maximum spectral intensity on axis.

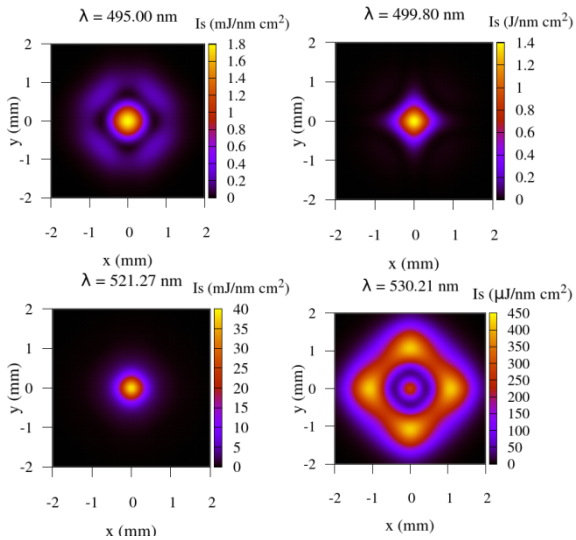

Figure 5: Transverse spectral intensity $I_s(x,y)$ for the wavelengths 495.0, 499.8, 521.3 and 530.2 nm. Note the difference in scale for $I_s(x,y)$ at the various frequencies.

So far, we have demonstrated the new diagnostics in the spectral domain. However, propagation in the frequency domain also allows the use of dispersive optical components along the optical path. For example, if we consider a multilayer mirror, then reflecting a short optical pulse from the mirror is problematic to implement in the time domain, as the pulse may temporally broaden. By transforming to the frequency domain and if the complex reflection coefficient (reflected amplitude and phase shift) of the mirror is available for the frequency range of interest (either measured or calculated), we can reflect each frequency component of the mirror. By transforming back to the time domain, the pulse has been reflected from the mirror including broadening of the pulse due to the partial reflection at the layers of the mirror. Alternatively, if the optical pulse propagates through a material, a wavelength dependent refractive index can be included.

CONCLUSION

We have described the enhanced capabilities of OPC. In particular, the in-line diagnostics are considerably faster than the off-line diagnostics and a single in-line diagnostic command hardly changes the runtime of a single propagation step. Only for a very large number of grid points and a larger number of time samples do the in-line diagnostics significantly add to the total run time. The waveguide modes that have been added are a first step towards guided propagation and towards interfacing with FEL gain codes that can handle partial or complete wave guiding. Finally, the transformation to the frequency domain allows for a more accurate propagation and introduces added diagnostics to the package. A propagation in the frequency domain also allows the use of dispersive optical elements.

Further extensions that are planned for the immediate future are the use of the HDF5 library for storing data to remain compatible with the upcoming release of GENESIS 1.3 and to implement a number of dispersive optical elements.

ACKNOWLEDGMENT

This work has been supported in part by the Office of Naval Research Global, grant number, N62909-10-1-7151.

REFERENCES

[1] S. Reiche, Nucl. Instr. Meth. A **429**, 243 (1999).
[2] W.M. Fawley, An Informal Manual for GINGER and its' post-processor XPLOTGIN, LBID-2141, CBP Tech Note-104, UC-414, 1995.
[3] H.P. Freund, Phys. Rev. E **52**, 5401 (1995).
[4] H.P. Freund et al., "Minerva, a new code to model free-electron lasers", TUP020, these proceedings, FEL'14, Basel, Switzerland (2014).
[5] J. Karssenberg et al., J. Appl. Phys. **100**, 093106 (2006).
[6] P.J.M. van der Slot et al., "Design of a resonator for the CSU THz FEL" in *Proc. 35th Int. Free-Electron Laser Conf.*, New York, pp. 719-722 (2013).
[7] See also G. Dattoli et al., "Free-electron laser oscillator: short pulses, mode locking, harmonic generation and tapering", WEA02, these proceedings, FEL'14, Basel, Switzerland (2014).

ISBN 978-3-95450-133-5